Available online at www.sciencedirect.com
SCIENCE DIRECT®
Journal of Power Sources 137 (2004) 288–308
JOURNAL OF POWER SOURCES
www.elsevier.com/locate/jpowsour

Influence of H_2SO_4 concentration on the mechanism of the processes and on the electrochemical activity of the $Pb/PbO_2/PbSO_4$ electrode

D. Pavlov*, A. Kirchev, M. Stoycheva, B. Monahov

Lead-Acid Batteries Department, Institute of Electrochemistry and Energy Systems (former CLEPS), Bulgarian Academy of Sciences, Sofia 1113, Bulgaria

Received 25 February 2004; received in revised form 6 May 2004; accepted 7 June 2004
Available online 31 July 2004

Abstract

The aim of the present investigation is to study the influence of H_2SO_4 concentration on the electrochemical activity, the phase composition and the structure and morphology of the PbO_2 particles. The study is performed through cycling (between 700 and 1600 mV versus Hg/Hg_2SO_4 electrode) of a $Pb/PbO_2/PbSO_4$ electrode immersed in sulfuric acid solutions of various concentrations (ranging within 2 orders of magnitude: 6.0–0.05 M H_2SO_4). In this concentration region, sulfuric acid dissociates in two steps resulting in the formation of HSO_4^- and SO_4^{2-} ions, respectively. It has been established experimentally that the electrochemical activity of the $PbO_2/PbSO_4$ electrode depends on the concentration of HSO_4^- ions in the solution. Three acid concentration regions can be distinguished: (a) active acid concentration region ($5.0\,M > C_{H_2SO_4} > 0.5\,M$), where the concentration of HSO_4^- ions is the highest and a βPbO_2 phase is formed; PbO_2 particles are drop-like in shape and contain large hydrated (gel) zones; the electrode has the highest capacity; (b) passive high concentration region ($C_{H_2SO_4} > 5.0\,M$), where the concentration of HSO_4^- ions decreases at the expense of formation of H_2SO_4 molecules; crystal-shaped αPbO_2 particles are formed; the capacity of the electrode declines; (c) passive low concentration region ($C_{H_2SO_4} < 0.5\,M$), where the concentration of HSO_4^- ions decreases at the expense of the formation of SO_4^{2-} ions; the content of αPbO_2 in the anodic layer increases; PbO_2 particles are crystal-shaped and are interconnected in dendrites; the capacity of the electrode declines. The above electrochemical behavior of the $PbO_2/PbSO_4$ electrode is explained by the mechanism of the reactions in the gel zones of the PbO_2 particles and by the influence of HSO_4^- ions on the number of electrochemically active particles. On grounds of the obtained experimental results it has been established that the working interval within which the $C_{H_2SO_4}$ may change on cycling is from 5.0 to 1.5 M, i.e. 3.5 M H_2SO_4 per 1 l of H_2SO_4 solution with s.g. 1.28 takes part in the reactions on both battery plates. This is the maximum amount of H_2SO_4 in the solution that would have no detrimental effect on the positive plates of the lead-acid battery.

Keywords: $PbO_2/PbSO_4$ electrode; PbO_2 reduction; $PbSO_4$ oxidation; PbO_2 structure; Lead-acid batteries; Lead-acid batteries charge processes; Lead-acid batteries discharge processes

1. Introduction

The cycle life of lead-acid batteries is often limited by softening, shedding and passivation of the lead dioxide active mass. The positive active material (PAM) is a porous mass. On battery cycling, reactions proceed as a result of which the H_2SO_4 concentration in the PAM pores increases on charge and decreases on discharge.

$$PbO_2 + H_2SO_4 + 2H^+ + 2e^- \Leftrightarrow PbSO_4 + 2H_2O \quad (1)$$

These changes in H_2SO_4 concentration in the pores of PAM may affect both the structure and morphology of the PbO_2 particles and agglomerates formed during charge as well as the morphology of the $PbSO_4$ crystals obtained during discharge [1–6].

Valve-regulated lead-acid batteries operate under conditions of slight deficiency of H_2SO_4 as a result of which, on deep discharge, the concentration of the H_2SO_4 in the plate pores drops down to very low values and the subsequent charge starts at this low concentration. On the other hand, in an attempt to compensate partially for the H_2SO_4 shortage, many VRLA battery manufacturers use H_2SO_4 solutions with concentrations higher than 1.28 s.g. At the end of charge the H_2SO_4 concentration in the plate pores is even higher than that of the solution initially filled into the battery. The question arises whether these extreme variations of the H_2SO_4 concentration in VRLAB allow the formation of

* Corresponding author. Tel.: +359 2 718651; fax: +359 2 731552.
E-mail address: dpavlov@mbox.cit.bg (D. Pavlov).

0378-7753/$ – see front matter © 2004 Elsevier B.V. All rights reserved.
doi:10.1016/j.jpowsour.2004.06.006

PbO_2 and $PbSO_4$ structures with high chemical and electrochemical activity, which would yield high battery capacity and long cycle life.

The processes of formation of the PbO_2 and $PbSO_4$ phases are complicated first by the two dissociation stages of H_2SO_4, which lead to formation of SO_4^{2-} and HSO_4^- ions. Secondly, the solubility of $PbSO_4$ crystals depends strongly on the H_2SO_4 concentration, which is responsible for the different concentration of Pb^{2+} ions in the pores of PAM depending on the state of charge and discharge [7,8]. Still another peculiarity is that the sulfuric acid ions adsorb onto the PbO_2 surface and thus influence the processes of PbO_2 phase formation [9–11]. And finally, Pb^{2+} ions form a number of complex ions depending on the pH of the solution [12]. It has been established that the H_2SO_4 concentration affects not only the electrode kinetics but also the maximum utilization of the active materials of the $Pb/PbO_2/PbSO_4$ electrode [13–17].

The processes of $PbSO_4$ oxidation to PbO_2 and of PbO_2 reduction to $PbSO_4$ involve the decomposition of one solid phase and the formation of a new solid phase. To disclose the relationship between the processes of decomposition of the initial phase and those of formation of the new phase is one of the aims of the present paper. The second aim is to determine the influence of H_2SO_4 concentration on the above processes. And finally, based on the fundamental results obtained, to draw a purely practical conclusion about the amount of H_2SO_4 that can be utilized during cycling with no adverse effect on the cycle life of the battery.

2. Experimental methods

2.1. Philosophy of the investigation

The mechanism of the processes of conversion of one solid phase into another one as a result of an electrochemical reaction can be disclosed if the electrochemical reaction proceeds at a high rate. In this case, some of the slow elementary processes will not proceed at all and the individual elementary reactions and the formation of intermediate products could be differentiated. The subsequent slow potential sweep provides information about the slow processes. In the present investigation we used linear scanning voltametry (LSV) at potential scan rate of 100 mV/s for the fast potential sweep and 2.0, 4.0 or 10.0 mV/s for the slow one.

We used sulfuric acid solutions with concentrations from 6.0 to 0.05 M H_2SO_4, i.e. the $C_{H_2SO_4}$ was varied within 2 orders of magnitude.

Based on the structure of the anodic layer formed and the morphology of the particles we can judge about the processes of nucleation and growth of the new phase as well as about the decomposition of the initial phase. For the purpose we performed exhaustive SEM examinations and the characteristic SEM pictures are presented in this paper. At magnifications higher than 40,000, we observed the PbO_2 particles and $PbSO_4$ nuclei (microstructure), and at lower magnifications, the interconnection of PbO_2 particles in agglomerates and aggregates (macrostructure).

2.2. Electrochemical cell and experimental set-up

A classical three-electrode glass cell was used comprising a smooth Pb (99.999%) working electrode, a Hg/Hg_2SO_4 reference electrode and a Pt counter-electrode. The anodic layer was obtained through cycling of the Pb electrode immersed in H_2SO_4 solution. Electrode polarization was conducted between 1600 and 700 mV (versus Hg/Hg_2SO_4 electrode), i.e. within the PbO_2 and $PbSO_4$ potential regions, at a scan rate of 100 mV/s. This technology allowed gradual formation of a PbO_2 anodic layer in the H_2SO_4 solution of a given concentration. After 1 or 16 h of cycling, the electrode was taken out of the solution and samples of the obtained anodic layer were examined in a scanning electron microscope. Its phase composition was determined through X-ray diffraction analysis.

Table 1 summarizes the values for the H_2SO_4 concentrations, as expressed in the chemical practice (*M*, mol/l) and in the battery industry (s.g.: specific gravity), respectively. Merck's data tables were used [18]. A more detailed description of the procedures used is presented in reference [6].

2.3. Dependence of the equilibrium potential of the $Pb/PbO_2/PbSO_4$ electrode on H_2SO_4 concentration

For H_2SO_4 concentrations higher than 0.5 M (pH < 1.0) the equilibrium potential of the $Pb/PbO_2/PbSO_4$ electrode can be represented by the following equation [19]:

$$PbO_2 + HSO_4^- + 3H^+ + 2e^- = PbSO_4 + 2H_2O \quad (2)$$

$$E = 1.628 - 0.88\,pH + 0.029 \log a_{HSO_4^-} \quad (2')$$

The potential is referred to a hydrogen electrode. The equilibrium potential of the $Pb/PbO_2/PbSO_4$ electrode depends on the pH of the H_2SO_4 solution. On varying the H_2SO_4 concentration from 5.0 to 0.05 M, the equilibrium potential shifts from 1258 to 787 mV (versus Hg/Hg_2SO_4 electrode). When cycled between 1600 and 700 mV the electrodes stay in the PbO_2 and $PbSO_4$ potential regions different periods of time as a result of which different amounts of PbO_2 and $PbSO_4$ phases are formed. In concentrated H_2SO_4 solutions the time of stay of the electrode in the $PbSO_4$ potential region will be longer than in the PbO_2 one, whereas at low H_2SO_4 concentrations the reverse situation is observed. The aim of the present investigation is to establish whether the changes in H_2SO_4 concentration lead to changes in the type and structure of the anodic layer, and in the morphology of the PbO_2 particles and their electrochemical activity, as well as in the morphology of the $PbSO_4$ crystals, i.e. purely qualitative changes.

Table 1
H_2SO_4 concentrations of the solutions used for the experiments [18]

M (mol/l)	6.0	5.0	2.81	2.06	1.56	0.86	0.5	0.18	0.05
Specific gravity of H_2SO_4	1.39	1.285	1.17	1.125	1.095	1.050	1.030	1.010	1.000
C (%)	44.17	37.95	23.95	18.09	14.04	7.704	4.756	1.731	0.49

3. Experimental results

3.1. Dependence of the amount of PbO_2 involved in the electrochemical reaction of reduction at the $Pb/PbO_2/PbSO_4$ electrode on H_2SO_4 concentration (electrochemical activity of PbO_2)

The amount of PbO_2 in the anodic layer that takes part in the electrochemical reduction was measured coulometrically and the results obtained were presented in the first announcement of these investigations [6]. The present paper provides some additional results. Fig. 1 presents the dependence of the electrochemical activity of PbO_2 (determined by the quantity of electricity flowing through the electrode on reduction of the PbO_2 layer at cathodic scan rate of 1 mV/s) on the H_2SO_4 concentration. The measurements were performed after 1 and 16 h of electrode cycling. Judging by the profile of the curves, three H_2SO_4 concentration regions can be identified:

(a) Passive high concentration region: This region includes concentrations higher than 5 M H_2SO_4. The anodic layer formed within this region has low electrochemical activity that decreases on further increase of the H_2SO_4 concentration.
(b) Active medium concentration region: Covering concentrations between 5.0 and 0.5 M H_2SO_4 and yielding an electrochemically active anodic layer. It is within this concentration region that the positive electrode of the lead-acid battery operates.
(c) Passive low concentration region: It includes concentrations below 0.5 M H_2SO_4. The anodic layer formed within this concentration region has low electrochemical activity that decreases with decrease of the H_2SO_4 concentration.

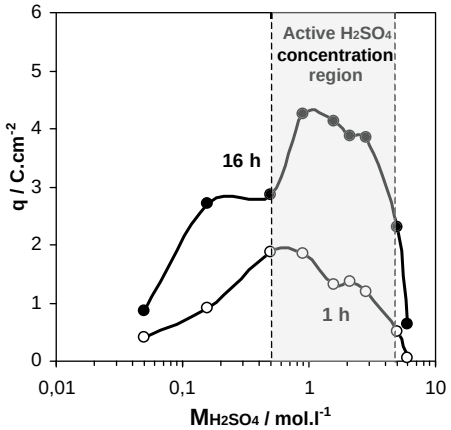

Fig. 1. Amount of active PbO_2 involved in the reduction process, as a function of H_2SO_4 concentration [6].

3.2. Phase composition of the anodic layer formed at various H_2SO_4 concentrations

The phase composition was determined through XRD analysis, from the areas of the characteristic diffraction peaks for βPbO_2 ($d = 0.350$ nm), $\alpha PbO_2 + tetPbO$ ($d = 0.313$ nm—this line is common for both phases, but it reflects mainly the content of αPbO_2), $PbSO_4$ ($d = 0.300$ nm) and Pb ($d = 0.284$ nm). The X-ray patterns give the phase composition of the surface sub-layer of the anodic layer that is in contact with the solution and this sub-layer was examined by scanning electron microscopy.

Fig. 2 presents the areas of the characteristic X-ray diffraction peaks reflecting the content of the individual crystal phases for the anodic layers formed in H_2SO_4 solutions

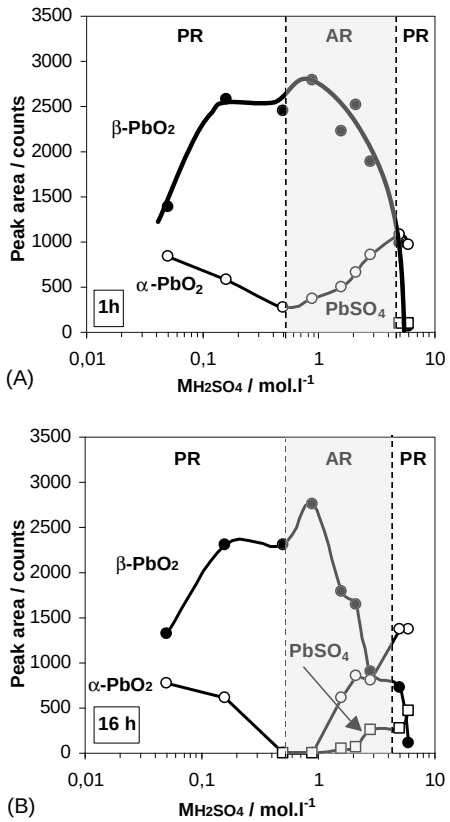

Fig. 2. Phase composition of the anodic layer formed for 1 h (a) and for 16 h of cycling (b) of a Pb electrode between 700 and 1600 mV at 100 mV/s vs. H_2SO_4 concentration.

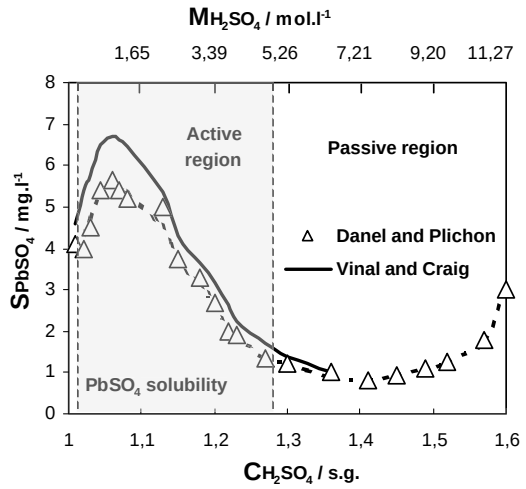

Fig. 3. Dependence of the solubility of $PbSO_4$ crystals on H_2SO_4 concentration, as determined by Vinal and Craig [7], and Danel and Plichon [8].

with concentrations varying between 6.0 and 0.05 M after 1 h (Fig. 2a) and 16 h (Fig. 2b) of cycling.

It is evident from Fig. 2a that, within the passive high concentration region ($C_{H_2SO_4}$ > 5.0 M H_2SO_4), the anodic layer contains mostly αPbO_2 and $PbSO_4$, and negligible amounts of βPbO_2.

In the active H_2SO_4 concentration region the amount of βPbO_2 in the anodic layer exceeds by several times that of the αPbO_2 phase. Below 0.86 M H_2SO_4 concentrations, the content of βPbO_2 decreases on further dilution of the H_2SO_4 solution.

In the passive region of low H_2SO_4 concentrations ($C_{H_2SO_4}$ < 0.5 M), the amount of αPbO_2 in the anodic layer increases, whereas that of βPbO_2 decreases. The reactions of αPbO_2 reduction to $PbSO_4$ and the subsequent oxidation to βPbO_2 are impeded. It is true that at these concentrations the electrode stays for a very short time within the $PbSO_4$ potential region, which may have its own effect on phase composition, too.

Comparing the data for the two passive regions it is worth noticing that great amounts of αPbO_2 form in both regions. In the active region mainly βPbO_2 is formed. A comparison between Figs. 1 and 2 suggests that the morphology of the PbO_2 crystals exerts an influence on its electrochemical activity.

3.3. Solubility of $PbSO_4$ crystals as a function of H_2SO_4 concentration

Fig. 3 presents the dependence of the solubility of $PbSO_4$ crystals on the concentration of H_2SO_4 as determined by Vinal and Craig [7], and Danel and Plichon [8].

In 5.0 M H_2SO_4 solution, the solubility of $PbSO_4$ crystals is low, about 1.8 mg/l. It almost doubles (4.1 mg/l) in 2.81 M H_2SO_4 solution and in the concentration region between 2.06 and 0.5 M H_2SO_4 the $PbSO_4$ solubility reaches its maximum value, 6.0–6.5 mg/l. On further decrease of the H_2SO_4 concentration the solubility of $PbSO_4$ decreases again.

On comparing Figs. 1–3 it can be seen that the solubility of $PbSO_4$ is the highest within the active zone of H_2SO_4 concentrations. The maximum amount of βPbO_2 formed in the anodic layer at 0.86 M H_2SO_4 concentration corresponds to the maximum solubility of the $PbSO_4$ crystals. In the passive zones of H_2SO_4 concentrations, $PbSO_4$ has but a low solubility, different in concentrated and diluted solutions.

3.4. Basic elements comprising the structure of the lead dioxide layer

When a lead electrode immersed in H_2SO_4 solution is polarized in the lead dioxide potential region (φ > equilibrium potential of the $Pb/PbO_2/PbSO_4$ electrode), the surface of the electrode is oxidized and a PbO_2 layer is formed. Let us call this layer primary PbO_2 layer.

On cycling, when the electrode potential becomes more negative than the equilibrium potential of the $Pb/PbO_2/PbSO_4$ electrode system, the primary layer is reduced to $PbSO_4$. Then during the anodic sweep, when the potential enters again the lead dioxide potential region, the $PbSO_4$ is oxidized to PbO_2. The secondary PbO_2 layer is formed.

Fig. 4 shows the elements building the structure of the anodic layer. These include:

(a) Individual particles (Fig. 4a): These particles are globular in shape. Most of the globules have almost spherical shape and some of them are elongated.
(b) Agglomerates (Fig. 4a and b): Several particles (10–15) interconnect to form an agglomerate. Agglomerates may be almost spherical, elongated or shapeless. The connections between the particles may vary from tightly adhering to each other with hardly visible inter-particle boundaries to well pronounced particles with clearly visible small contact surfaces between them.
(c) Aggregates (Fig. 4b): Numerous agglomerates and particles interconnect to form aggregates. The latter may be shapeless and microporous in structure.

These are the basic elements building the structure of the anodic layer formed on oxidation of a smooth electrode. An analogous structure has been established also in the positive active mass [20,21]. In fact, through cycling the Pb electrode for 1 or 16 h we form positive active mass by the Gaston Planté method.

3.5. Structure of the anodic layer formed in the passive high acid concentration region

(a) 5 M H_2SO_4 solution (1.28 s.g.): The SEM pictures in Fig. 5 show the anodic layer after 1 h of electrode cycling, whereby electrode polarization was stopped at 1600 mV. The pictures feature:

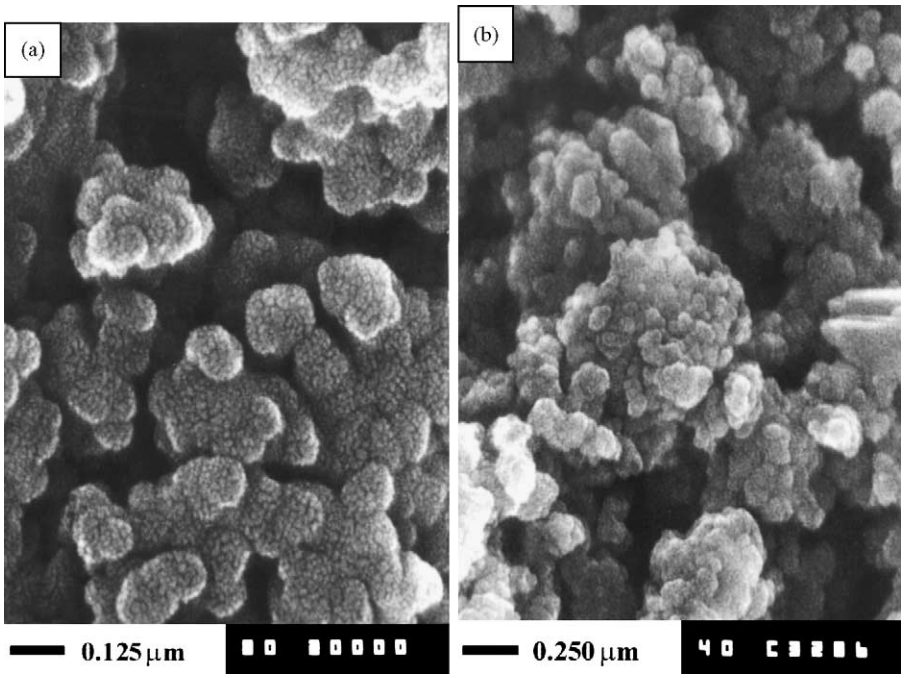

Fig. 4. Building elements of the structure of the PbO_2 anodic layer.

- Zones of compact continuous passive layer comprising tightly interconnected almost spherical PbO_2 particles with no pores in-between (Fig. 5a); These zones have probably formed during the initial anodic oxidation of lead and they present the primary anodic layer. This layer is passive and participates but weakly in the charge–discharge processes.
- Zones of loose structure with well shaped PbO_2 particles and micropores between some of the particles (Fig. 5b); These zones in the anodic layer are involved in the cycling processes and probably contain βPbO_2 particles.

The anodic layers obtained after 1 and 16 h of cycling do not differ much in structure, except for the increased size of the zones of loose structure on continuous electrode cycling.

Fig. 6 presents pictures of the anodic layer formed after 1 h of cycling of the electrode whose cathodic polarization was stopped at 700 mV, i.e. in the $PbSO_4$

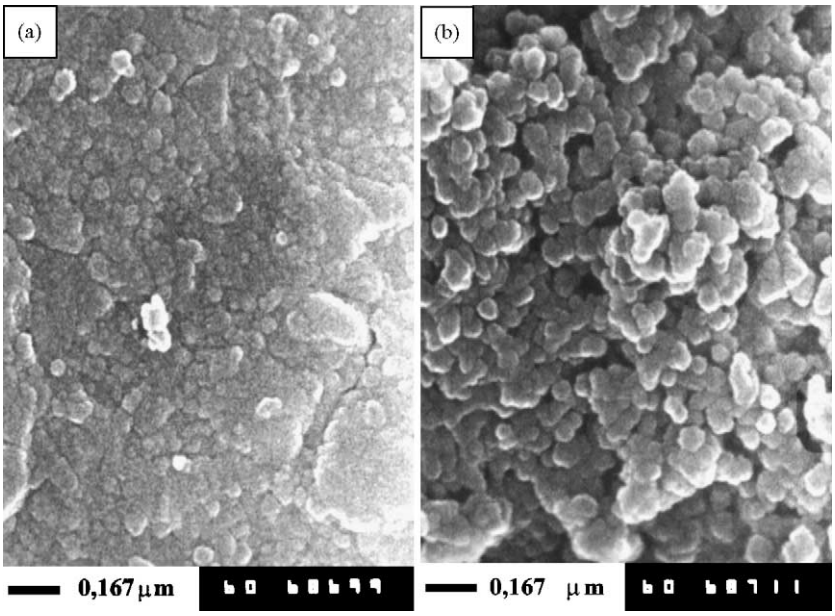

Fig. 5. Anodic layer formed after 1 h of cycling of a $Pb/PbO_2/PbSO_4$ electrode in 5 M H_2SO_4 solution. Electrode polarization was stopped at 1600 mV vs. Hg/Hg_2SO_4 reference electrode.

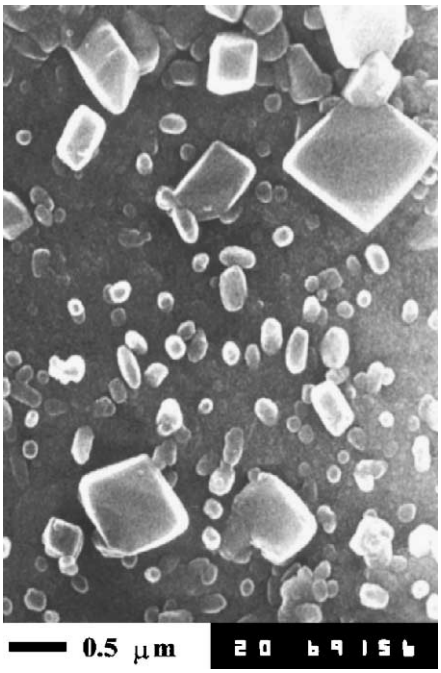

Fig. 6. Anodic layer formed after 1 h of cycling of a $Pb/PbO_2/PbSO_4$ electrode in 5 M H_2SO_4 solution. Polarization was stopped at 700 mV, whereby part of the PbO_2 has been reduced and $PbSO_4$ nuclei and crystals have formed.

potential region. $PbSO_4$ nuclei (sized between 80 and 150 nm) and $PbSO_4$ crystals (about 1 μm) had formed at some sites on the PbO_2 surface. This indicates that the reduction of PbO_2 proceeds in active centers. As the $PbSO_4$ nuclei differ in size, it may be expected that these active centers will have different activity on PbO_2 reduction.

(b) 6 M H_2SO_4 solution (1.34 s.g.): Fig. 7 presents SEM micrographs of the anodic layer formed after 1 h of electrode cycling, whereby the polarization was stopped at 1600 mV. Crystal-shaped PbO_2 particles of two sizes are observed: (i) 80–100 nm, and (ii) larger than 150–200 nm. The PbO_2 particles cover uniformly the lead surface. Small aggregates of crystal-shaped well differentiated PbO_2 particles (80-100 nm) can be seen here and there (Fig. 7a). Probably, these have formed as a result of oxidation of the $PbSO_4$ crystals, whereby the obtained aggregates have not preserved fully the matrix of the $PbSO_4$ crystals. On comparing Figs. 5b and 7b it can be seen that in 5 M H_2SO_4 solution the PbO_2 particles are round or oval in shape, whereas those formed in 6 M H_2SO_4 solution have crystal shapes.

Fig. 8 shows pictures of the anodic layer formed after 16 h of electrode cycling in 6 M H_2SO_4 solution, whereby the polarization was stopped at 1600 mV (Fig. 8a and b) or at 700 mV (Fig. 8c and d). At this acid concentration, the reduction of PbO_2 particles yields flat prismatic $PbSO_4$ crystals with well shaped walls, edges and apexes (Fig. 8d). Part of these crystals remains unoxidized for the short time of stay of the electrode within the PbO_2 potential region (Fig. 8b). The low solubility of the $PbSO_4$ crystals contributes, too. The XRD analysis of the anodic layer formed on the electrode when its polarization was stopped at 1600 mV (Fig. 2) indicates that it is composed mainly of αPbO_2 and contains considerable amounts of $PbSO_4$ crystals and very small amounts of βPbO_2. An interesting

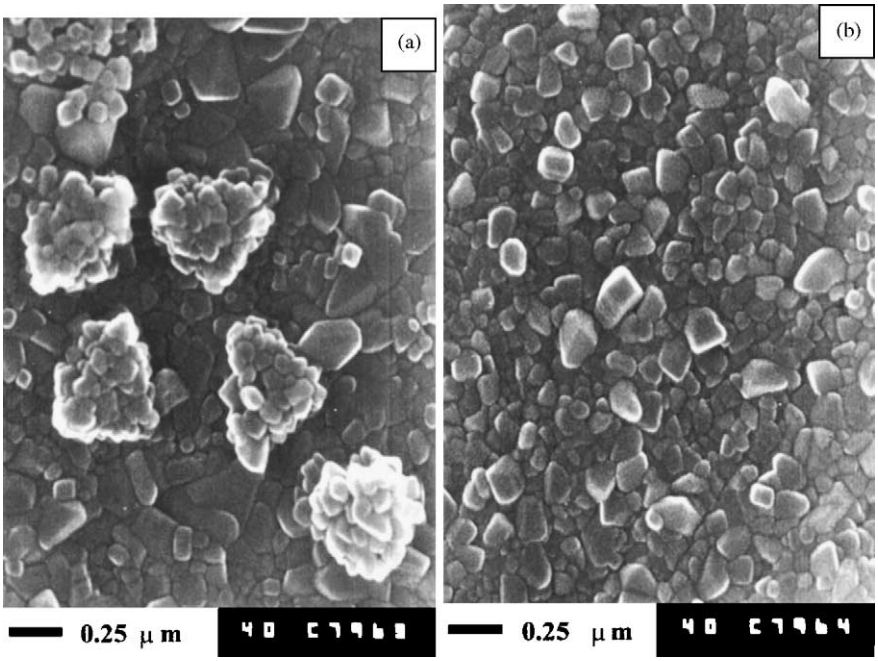

Fig. 7. Structure of the anodic layer formed after 1 h of cycling of a $Pb/PbO_2/PbSO_4$ electrode in 6 M H_2SO_4 solution. Electrode polarization was stopped at 1600 mV.

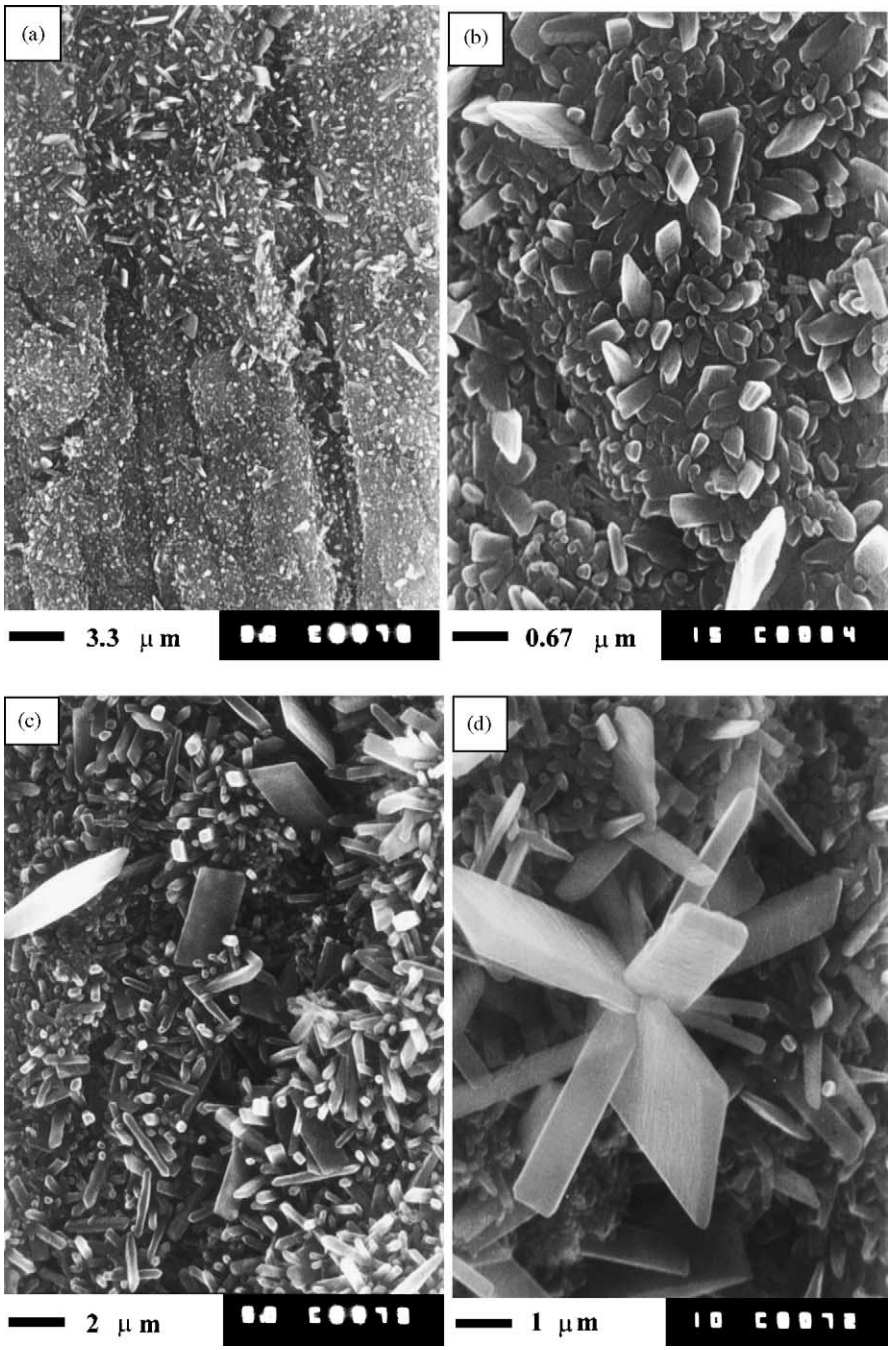

Fig. 8. Macro (a and c) and microstructure (b and d) of the anodic layer formed after 16 h of cycling of a $Pb/PbO_2/PbSO_4$ electrode in 6 M H_2SO_4 solution. Electrode polarization was stopped at: 1600 mV (a and b) and 700 mV (c and d).

finding is that the αPbO_2 phase is formed in strongly acidic medium and its particles have well pronounced crystal shapes.

3.6. Cycling of Pb electrodes in the active H_2SO_4 concentration region

After switching on the potentiostat a certain time is needed for reaching the pre-set potential (1600 mV), which time depends on the response time of the potentiostat. During this period, a very strong current flows through the electrode determined by the first electrochemical reaction of Pb oxidation to Pb^{2+}. A passive layer of $PbSO_4$ is formed. Then the potential increases rapidly and exceeds the equilibrium potential of the $Pb/PbO_2/PbSO_4$ electrode. The $PbSO_4$ layer is oxidized to PbO_2. The processes involved in the oxidation have been discussed earlier [22,23]. The type and amount of the initially formed $PbSO_4$ phase will

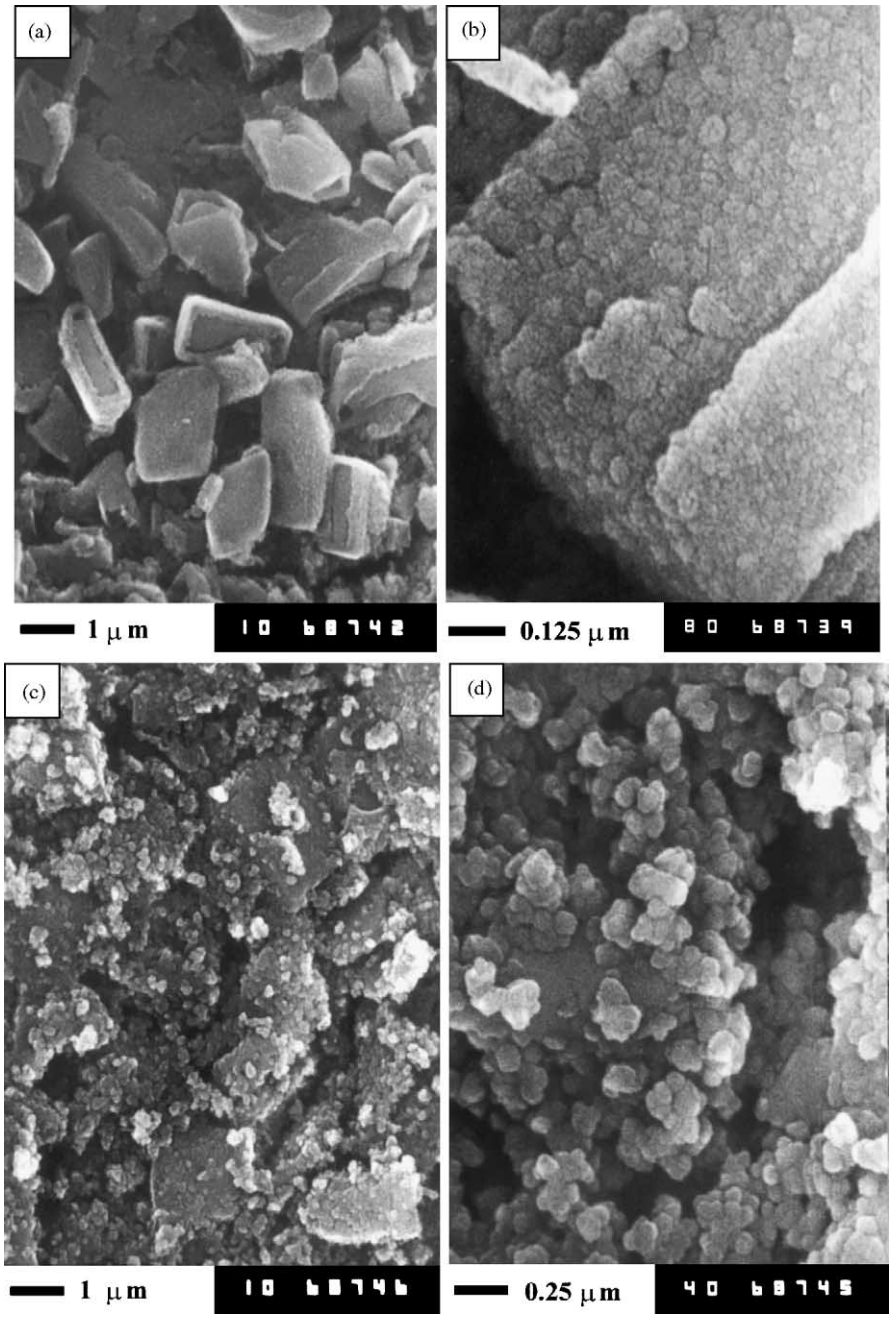

Fig. 9. Structure of the anodic layer formed after 1 h (a and b) and after 16 h (c and d) of cycling of a $Pb/PbO_2/PbSO_4$ electrode in 2.86 M H_2SO_4 solution.

depend on the solubility of $PbSO_4$ in the H_2SO_4 solution as well as on the rates of $PbSO_4$ nucleation and crystal growth.

In our experiment the time for reaching 1600 mV was about 3 ms. After 10 s of polarization at 1600 mV, electrode cycling began between 1600 and 700 mV, thus allowing the secondary anodic structure to form.

(a) 2.81 M H_2SO_4 (1.17 s.g.): Fig. 9 presents SEM pictures of the macro (Fig. 9a) and micro (Fig. 9b) structure of the anodic layer after 1 h of cycling. It can be seen from Fig. 9a that a considerable part of the $PbSO_4$ crystals have oxidized through a metasomatic process and the shape of the initial $PbSO_4$ matrix has been preserved. Let us call these PbO_2 aggregates metasomatic ones. They are built of globular PbO_2 particles sized 50–60 nm (Fig. 9b).

Fig. 9c and d presents the structure of the anodic layer formed after 16 h of electrode cycling. Some of the metasomatic PbO_2 aggregates have fully disintegrated as a result of cycling and the obtained PbO_2 particles have formed shapeless agglomerates (Fig. 9d) or have

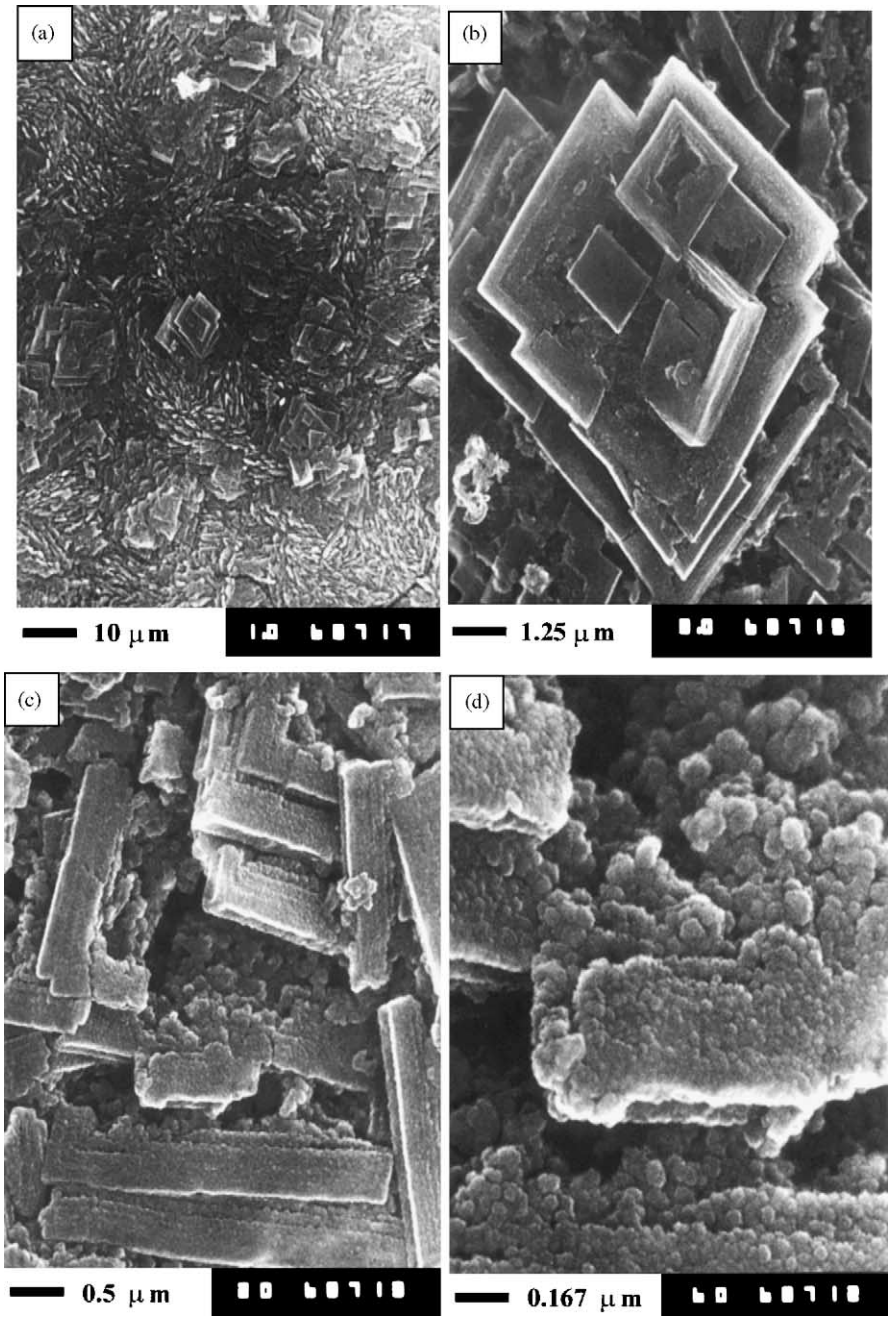

Fig. 10. Structure of the anodic layer formed after 1 h of cycling of a $Pb/PbO_2/PbSO_4$ electrode in 1.58 M H_2SO_4 solution. Long thin and flat rhombic or rectangular metasomatic aggregates built up of PbO_2 particles have formed.

precipitated on the surface of the PbO_2 metasomatic aggregates (Fig. 9c).

(b) 1.56 M H_2SO_4 (1.095 s.g.): At this acid concentration, the solubility of $PbSO_4$ crystals is the highest (Fig. 3) and the anodic layer formed is composed mostly of βPbO_2 (Fig. 2). Fig. 10 presents pictures of the anodic layer obtained after 1 h of electrode cycling. The photographs feature long thin (Fig. 10c) and flat rhombic or rectangular metasomatic aggregates of PbO_2 particles. Fig. 10b presents a picture of a rhombic metasomatic PbO_2 aggregate. These aggregates are flat and grow one over the other. They are thin, because they have formed within a thin reaction layer near the lead surface. In this layer the flows of Pb^{2+} ions meet with the SO_4^{2-} ions coming from the solution [24]. A reaction of $PbSO_4$ formation proceeds, which results in $PbSO_4$ crystal growth. Depending on the intensity and the direction of the Pb^{2+} ion flow, $PbSO_4$ crystals of different shapes are formed. When the electrode potential enters the PbO_2 potential region, these $PbSO_4$ crystals are oxidized to PbO_2 metasomatic aggregates. During electrode cycling, destruction of the metasoamtic rhombic aggregates starts in

their inner zones and advances towards the outer walls of the metasomatic aggregate. Fig. 10d shows SEM pictures of metasomatic PbO_2 aggregates at higher magnifications. The aggregates are built of globular PbO_2 particles sized from 40 to 50 nm. These are arranged in lines thus forming a wall or an edge.

Elongated and rhombic $PbSO_4$ crystals oxidize completely to PbO_2 metasomatic aggregates during electrode cycling. This is confirmed by the XRD data. Fig. 10 illustrates the oriented growth of the new PbO_2 phase, which is built up of PbO_2 particles arranged in rows (Fig. 10c and d). The crystal lattice of $PbSO_4$ influences strongly the arrangement of the PbO_2 particles in the newly formed layers of PbO_2 phase (Fig. 10b and c).

When a crystal (new phase) grows onto the surface of another crystal (substrate) and the crystal structure of the substrate affects or orients the crystal lattice of the new phase, the phenomenon is known as epitaxy. A similar phenomenon is observed when the $PbSO_4$ crystal is oxidized to PbO_2 metasomatic aggregate, but in this case, the new PbO_2 phase grows towards the interior of the substrate (the $PbSO_4$ crystal). The latter crystal contributes to the process by exerting an orienting effect on the arrangement of the newly formed PbO_2 particles into aggregates (Figs. 9b and 10). Let us call this phenomenon endotaxy, and the obtained oriented layers of PbO_2 particles in the aggregate, endotaxial layers. During battery charge, endotaxy plays an important role in building the structure of the positive active mass.

3.7. Pb electrodes cycled in the passive low acid concentration region

(a) 0.5 M H_2SO_4 (1.030 s.g.): Fig. 11 (1 h of electrode cycling) presents pictures illustrating the stages of disintegration of the metasomatic aggregates obtained after oxidation of the initially formed $PbSO_4$ crystals. The pictures in Fig. 11a and b feature a macrostructure comprising long plate-like aggregates of PbO_2. It can be seen from Fig. 11c that the sizes of the PbO_2 particles depend on the method of their formation. If formed as a result of metasomatic oxidation of the $PbSO_4$ crystals, these particles are spherical in shape, sized between 50 and 80 nm, and tightly adhering to each other thus forming a film. A closer look at their arrangement evidences linear endotaxial chains. Fig. 11c (bottom right hand side of the picture) shows also that the newly formed (secondary) PbO_2 particles, over the shapeless microporous aggregates, are larger in size (between 160 and 180 nm) and better shaped, i.e. the disintegration of the metasomatic aggregates on cycling is associated with changes in size, and probably also in structure and composition, of the PbO_2 particles and their connection into agglomerates and aggregates. Hence, the formation of PbO_2 particles proceeds through two different mechanisms depending on the precursor from which they originate.

The process of disintegration of the endotaxial PbO_2 layers is clearly illustrated in the pictures of the anodic layer presented in Fig. 11d–f. The interconnection of PbO_2 particles in linear chains, not only on the surface but also in the interior of the aggregate, is clearly visible in these pictures (Fig. 11e and f). Disintegration of the metasomatic aggregates proceeds through detachment of the linear chains from the aggregate. This implies that the binding energy of the PbO_2 particles in the chain is sufficiently strong to keep the chain intact and prevent it from disintegration.

Fig. 12a and b presents SEM pictures of the anodic layer formed after 16 h of electrode cycling at polarization up to 1600 mV. As a whole, the metasomatic aggregates have been destroyed completely and a shapeless microporous mass has formed. At this H_2SO_4 concentration disintegration of the metasomatic aggregates proceeds faster than in more concentrated solutions. Fig. 12c and d shows the structure of the anodic layer formed after 16 h of electrode cycling whereby the polarization was stopped at 700 mV. Single $PbSO_4$ crystals are formed here and there between the PbO_2 agglomerates. The obtained $PbSO_4$ crystals are sized between 0.2 and 1.0 μm and have cubic or prismatic shapes. During the subsequent anodic sweep, when the electrode potential enters the region of PbO_2 stability, $PbSO_4$ crystals are oxidized. Metasomatic processes depend on the concentration of H_2SO_4 and proceed only in $PbSO_4$ crystals greater than a certain critical size. When the size of the $PbSO_4$ crystals is smaller than this critical value, they form shapeless agglomerates.

(b) 0.18 M H_2SO_4 solution (1.010 s.g.): Fig. 13 presents pictures of the structure of the anodic layer and the morphology of the PbO_2 particles after 1 h of electrode cycling. There are no metasomatic PbO_2 aggregates and the secondary structure consists of layers of particles as well as elongated prismatic aggregates with cross-section 1.5 μm × 2.0 μm (Fig. 13b and c). The latter are composed of globular particles sized between 60 nm (spherical) and 160 nm (elongated) (Fig. 13c). The picture in Fig. 13b features some shapeless aggregates as well. PbO_2 particles are formed there in rows and the band grows towards the bulk of the solution. Some of the PbO_2 particles are arranged in layers (Fig. 13b and c), thus forming a layered prismatic aggregate (Fig. 13c).

Fig. 13d–f presents pictures of another $Pb/PbO_2/PbSO_4$ electrode cycled 1 h in 0.18 M H_2SO_4 at a scan rate of 100 mV/s. The PbO_2 particles are flat, 200 nm in size and are either single or several of them interconnect to form a flat agglomerate.

After 16 h of cycling, the anodic layer contains zones of shapeless microporous agglomerates (Fig. 14a and b) and dendrites in other zones (Fig. 14c and d). The

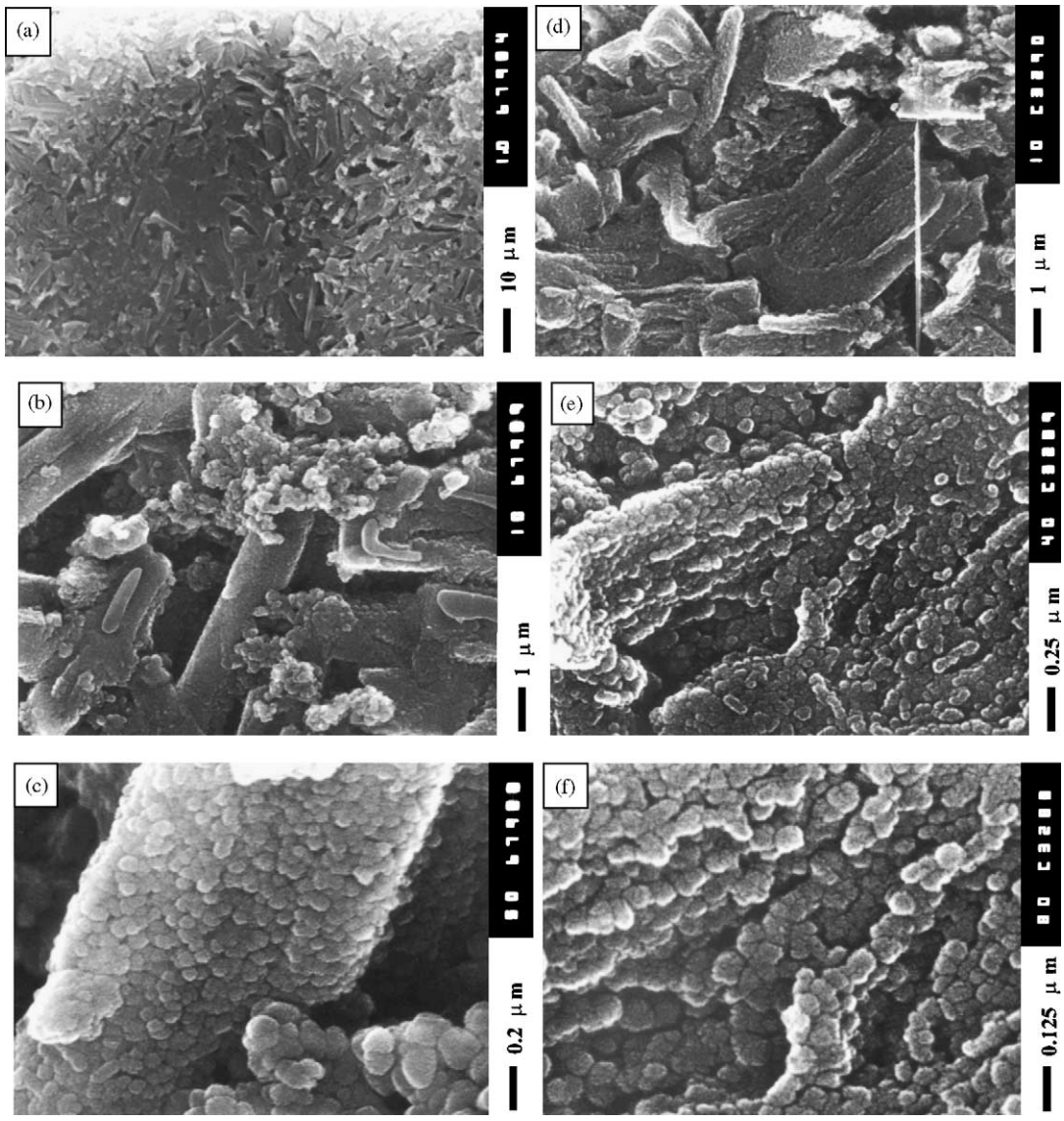

Fig. 11. Structure of the anodic layer formed after 1 h of cycling of a $Pb/PbO_2/PbSO_4$ electrode in 0.5 M H_2SO_4 solution. (d–f) Illustrates the disintegration of PbO_2 metasomatic aggregates.

dendrites are 10–20 μm in length and 2.0–2.5 μm in diameter. They are built of tightly interconnected PbO_2 particles with sizes between 100 and 150 nm (Fig. 14d).

(c) 0.05 M H_2SO_4 solution. Fig. 15 presents pictures of the secondary PbO_2 layer obtained after 1 h of cycling. The dendrites grow from certain sites of the primary PbO_2 layer (Fig. 15a and b). The pictures feature secondary branches in some parts of the dendrites and individual PbO_2 particles with crystal shape in other parts. Fig. 15c and d presents pictures of the anodic layer formed after 1 h of electrode cycling, whereby the polarization was stopped after reduction of PbO_2 at 700 mV. Cubic and prismatic $PbSO_4$ crystals are formed both over the primary anodic layer and over the dendrites. The formation of dendrites is fully manifested after 16 h of electrode cycling.

3.8. Influence of potential scan rate on the processes of dendrite formation

At the above low acid concentrations the solution is not buffered and its pH at the electrode surface can change, depending on the potential scan rate and on the ion diffusion hindrances, and may approach the neutral region. Close to and within this pH range, hydrolysis of Pb^{2+} ions proceeds as well as formation of a number of complex ions of the type $[Pb(OH)]^+$, $[Pb_3(OH)_4]^{2+}$, $[Pb_3(OH)_5]^+$, $[Pb_4(OH)_4]^{4+}$ and $[Pb_6(OH)_8]^{4+}$ [12].

If the above hypothesis about the influence of complex ions on the shape of the PbO_2 aggregates is true, then the potential scan rate should influence the shape of the agglomerates. Potential sweeps were conducted within the same potential range, 700–1600 mV at scan rates 2, 4, 10

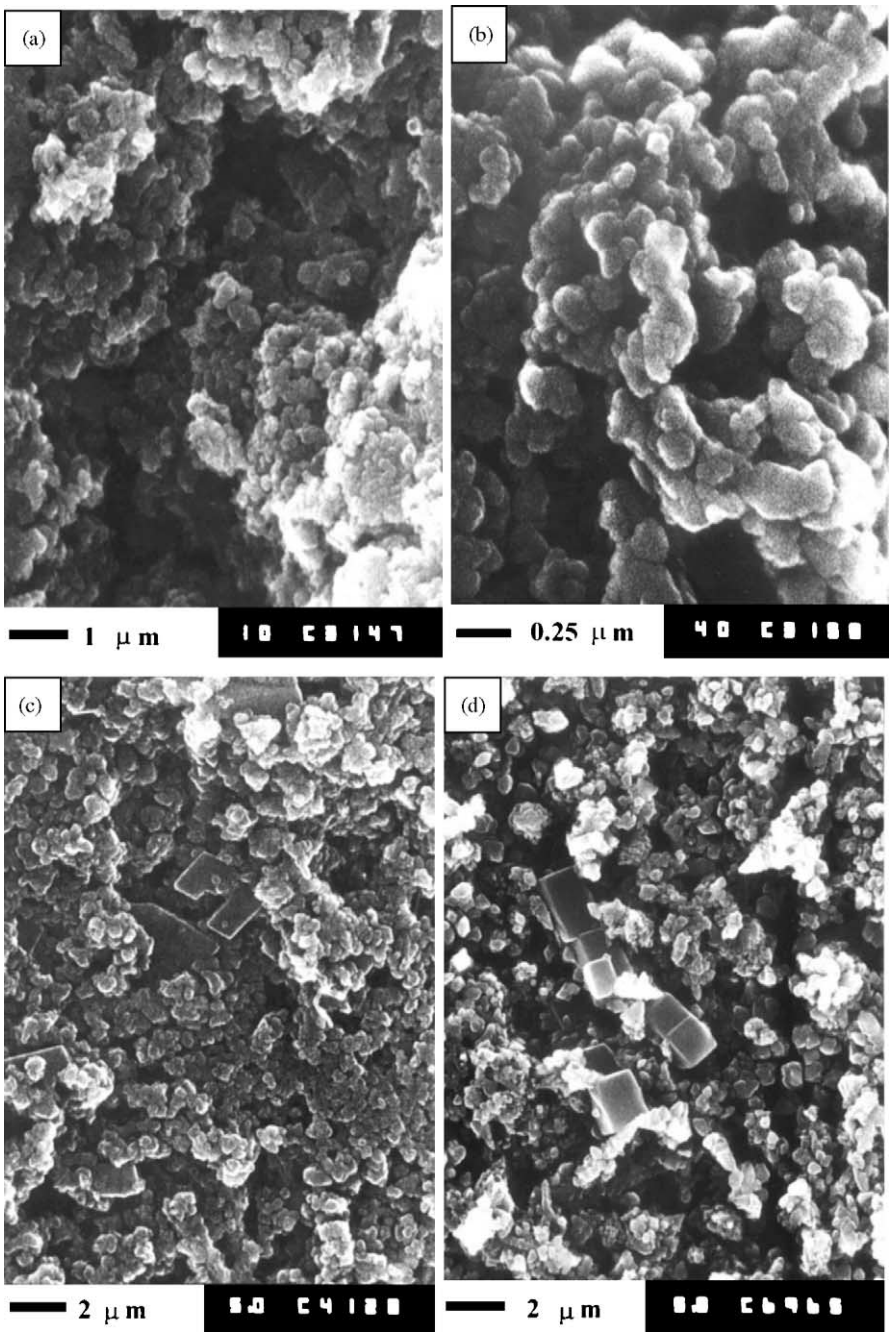

Fig. 12. Micro and macro structure of the anodic layer formed after 16 h of cycling of a $Pb/PbO_2/PbSO_4$ electrode in 0.5 M H_2SO_4 solution. Electrode polarization was stopped at 1600 mV (a and b) and at 700 mV (c and d).

or 20 mV/s for 1, 2 or 16 h of electrode cycling in 0.05 M H_2SO_4 solution. Fig. 16a and b shows pictures of the anodic layer after 16 h of electrode cycling at 2 mV/s, whereby the polarization was stopped at 1600 mV (Fig. 16a) and at 700 mV (Fig. 16b), respectively. The electrode stayed 87 s within the $PbSO_4$ potential region and 813 s within the PbO_2 potential region. At this potential scan rate no dendrites are formed and many of the PbO_2 particles have crystal shapes. The reduction of PbO_2 proceeds in active centers where cubic $PbSO_4$ crystals are formed (Fig. 16b). The latter are similar to the $PbSO_4$ crystals presented in Fig. 15c and d.

At potential scan rate 4 mV/s, the electrode stays 44 s in the $PbSO_4$ potential region and 406 s in the PbO_2 potential region (Fig. 16c and d). After 16 h of cycling, small dendrites are observed here and there in the anodic layer. This can be seen in the picture presented in Fig. 16c for electrode polarization up to 1600 mV. It is evident from the Fig. 16d that most of the dendrites have been reduced and $PbSO_4$ crystals have formed.

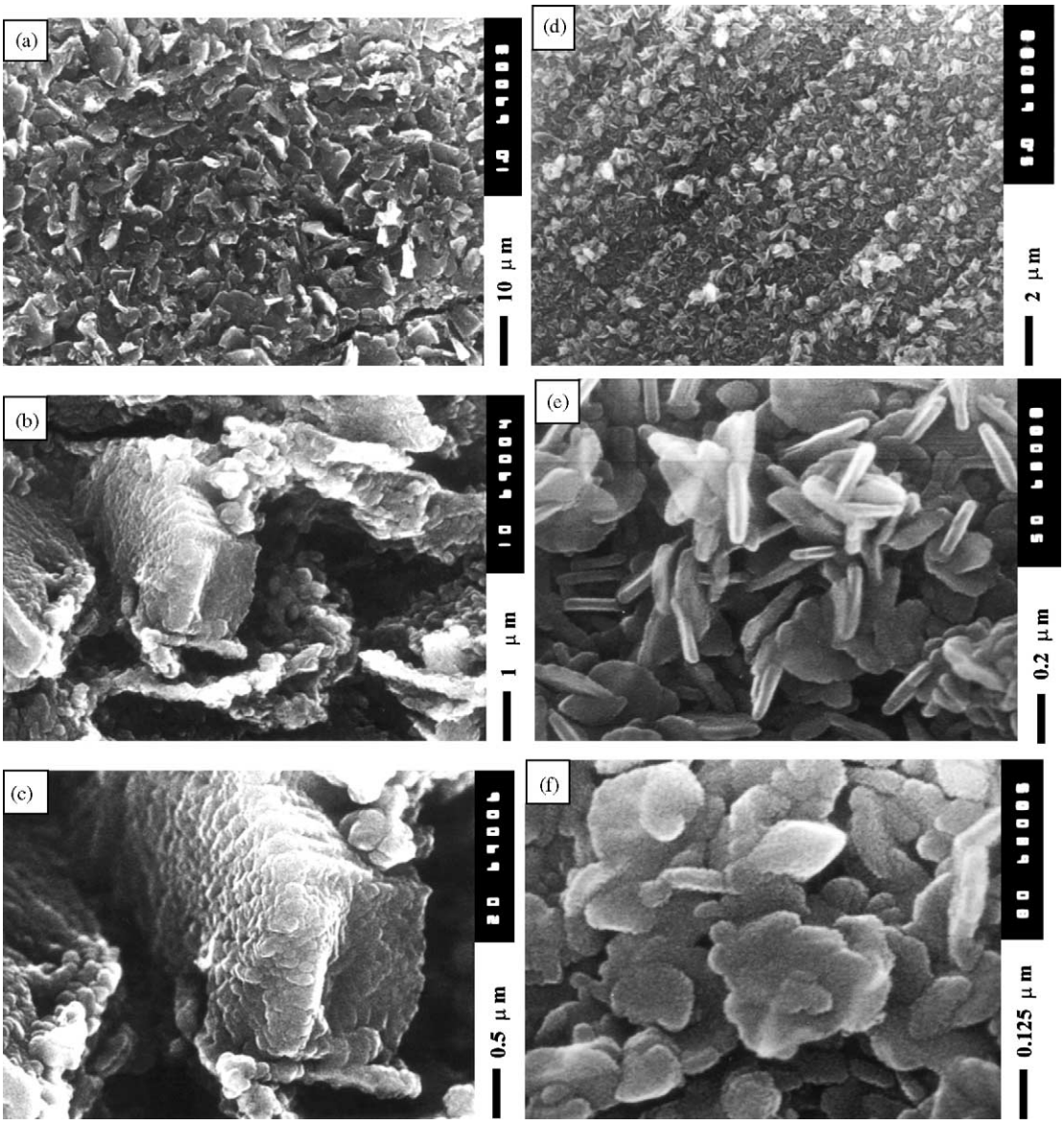

Fig. 13. Structure of the anodic layer formed after 1 h of cycling of a $Pb/PbO_2/PbSO_4$ electrode in 0.18 M H_2SO_4 solution. The anodic layer comprises thin layers of particles and elongated prismatic aggregates (c), or flat particles, single or interconnected into flat agglomerates (e and f).

Fig. 17 shows pictures of the anodic layer formed after 16 h of electrode cycling at 10 mV/s (Fig. 17a and b) and at 20 mV/s (Fig. 17c and d). Many of the dendrites formed at both scan rates are wide, step-like geometric formations, with frames on both sides of the dendrite (Fig. 17b and c).

The pictures in Fig. 17d evidence that the dendrites are built of small crystal-like particles arranged in rows. The primary anodic layer is relatively uniform and is composed of PbO_2 particles with crystal-like shapes (Fig. 17a and c).

On comparing Figs. 14, 15 and 17 is becomes evident that the shape of the dendrites and their structure change with changes in the H_2SO_4 concentration and in the potential scan rate.

The above results indicate that the algorithms of charge and discharge as well as the concentration of the H_2SO_4 solution are of utmost importance and determine the structure and electrochemical activity of the $Pb/PbO_2/PbSO_4$ electrode. Recently, pulse charge algorithms have been employed for lead-acid batteries for electric vehicle applications. The results of the present investigation evidence that the pulse charge mode, at certain H_2SO_4 concentrations, has a strong influence on the structure of the PbO_2 particles, agglomerates and aggregates, which in turn would affect the

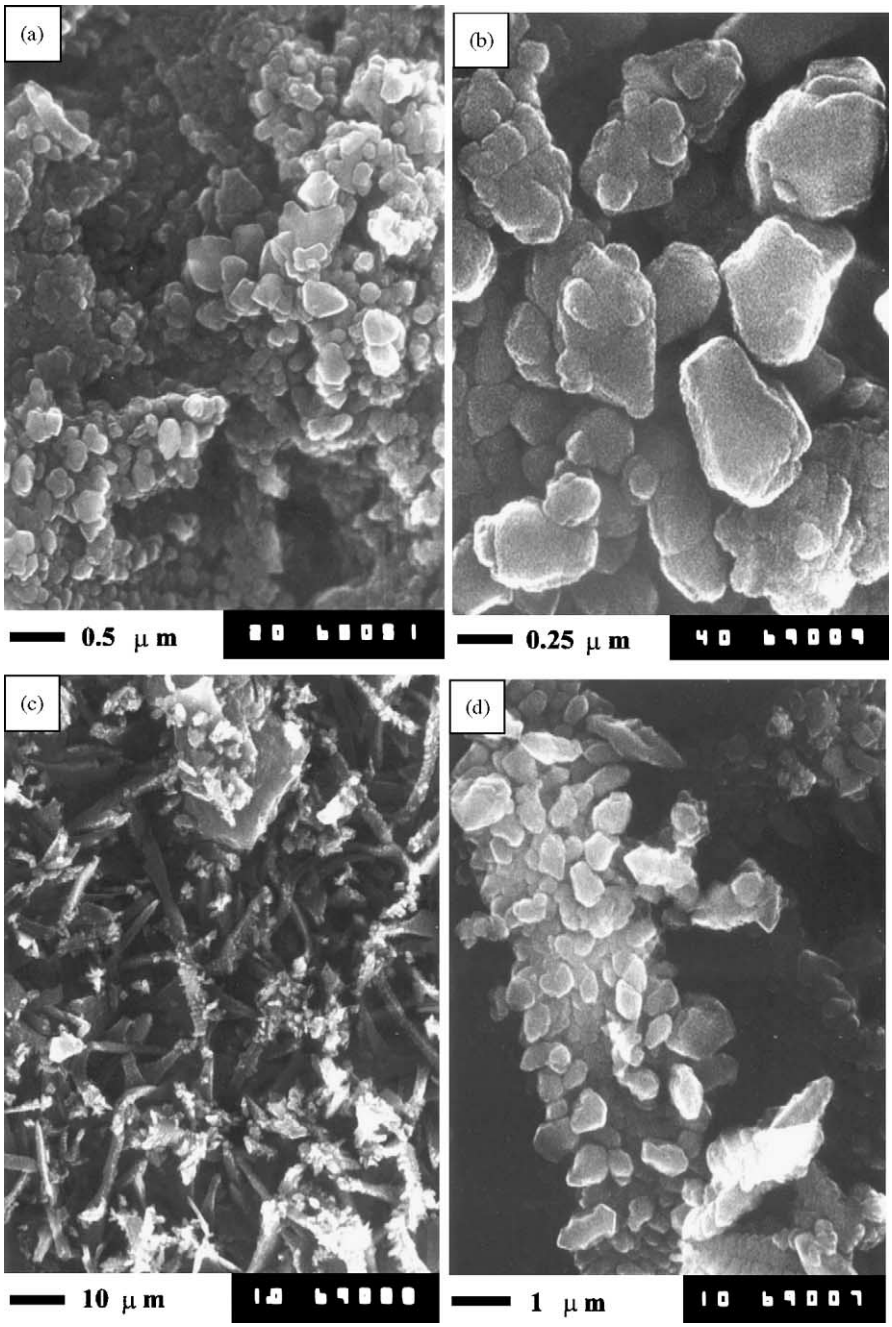

Fig. 14. Structure of the anodic layer formed after 16 h of cycling of a $Pb/PbO_2/PbSO_4$ electrode in 0.18 M H_2SO_4 solution.

electrochemical activity and cycle life of the lead-acid batteries.

4. Discussion of results

4.1. Dissociation of H_2SO_4 and its effect on the electrochemical activity of PbO_2

The question arises whether the observed diversity in structure of the anodic layer could be a function of the changes in a single parameter? We assumed that this parameter is the electrolyte composition.

The dissociation of sulfuric acid proceeds in two steps:

$$H_2SO_4 + H_2O = H_3O^+ + HSO_4^- \quad (3)$$

$$k_1 = \frac{a_{H_3O^+} a_{HSO_4^-}}{a_{H_2O} a_{H_2SO_4}} \quad (3')$$

According to Young and Blatz [25], $k_1 = 10^3$. In its first step of dissociation, H_2SO_4 is a strong acid.

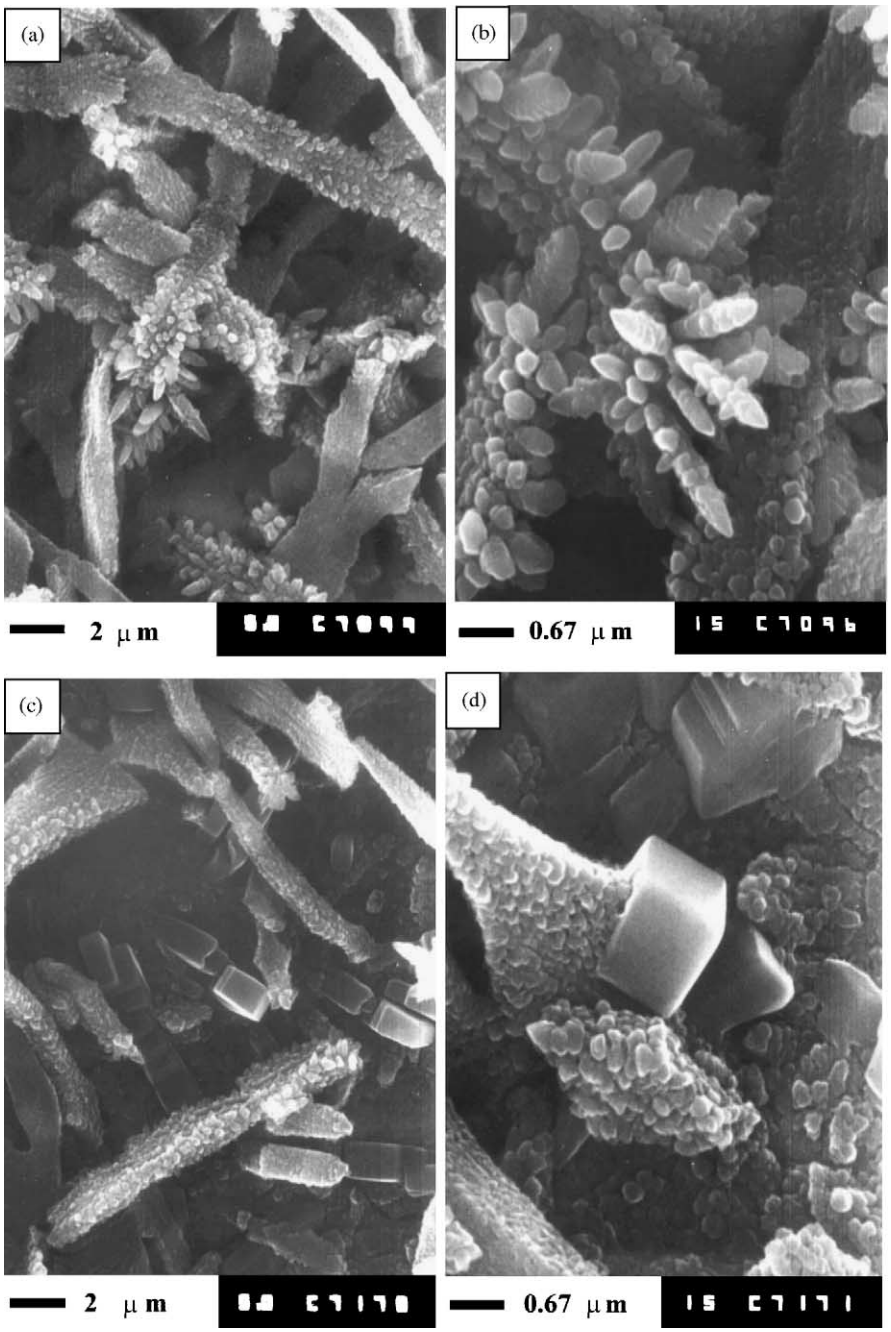

Fig. 15. Structure of the anodic layer formed after 1 h of cycling of a $Pb/PbO_2/PbSO_4$ electrode in 0.05 M H_2SO_4 solution. Electrode polarization was stopped at 1600 mV (a and b) and at 700 mV (c and d). The secondary anodic layer consists of dendrites unlike the primary layer which is built of crystal-shaped PbO_2 particles.

The second step of the dissociation is:

$$HSO_4^- = H^+ + SO_4^{2-} \quad (4)$$

$$k_2 = \frac{a_{H^+} a_{SO_4^{2-}}}{a_{HSO_4^-}} \quad (4')$$

According to Covington et al. [26], $k_2 = 0.0102$ ($pk_2 = 1.98$).

The ratio between the concentrations of H_2SO_4 molecules and HSO_4^- and SO_4^{2-} ions in the solution is thermodynamically determined by the equilibrium constants and depends on the concentration of H_2SO_4 in the system H_2SO_4/H_2O. Fig. 18 shows the changes in concentration of the above components as a function of the H_2SO_4 concentration, according to literature data [26–30]. The same figure gives also the three acid concentration regions established by us within which PbO_2 has different electrochemical activity.

On comparing Figs. 1 and 2 with Fig. 18 we can draw the following conclusion. The curve reflecting the dependence of the concentration of HSO_4^- ions versus H_2SO_4

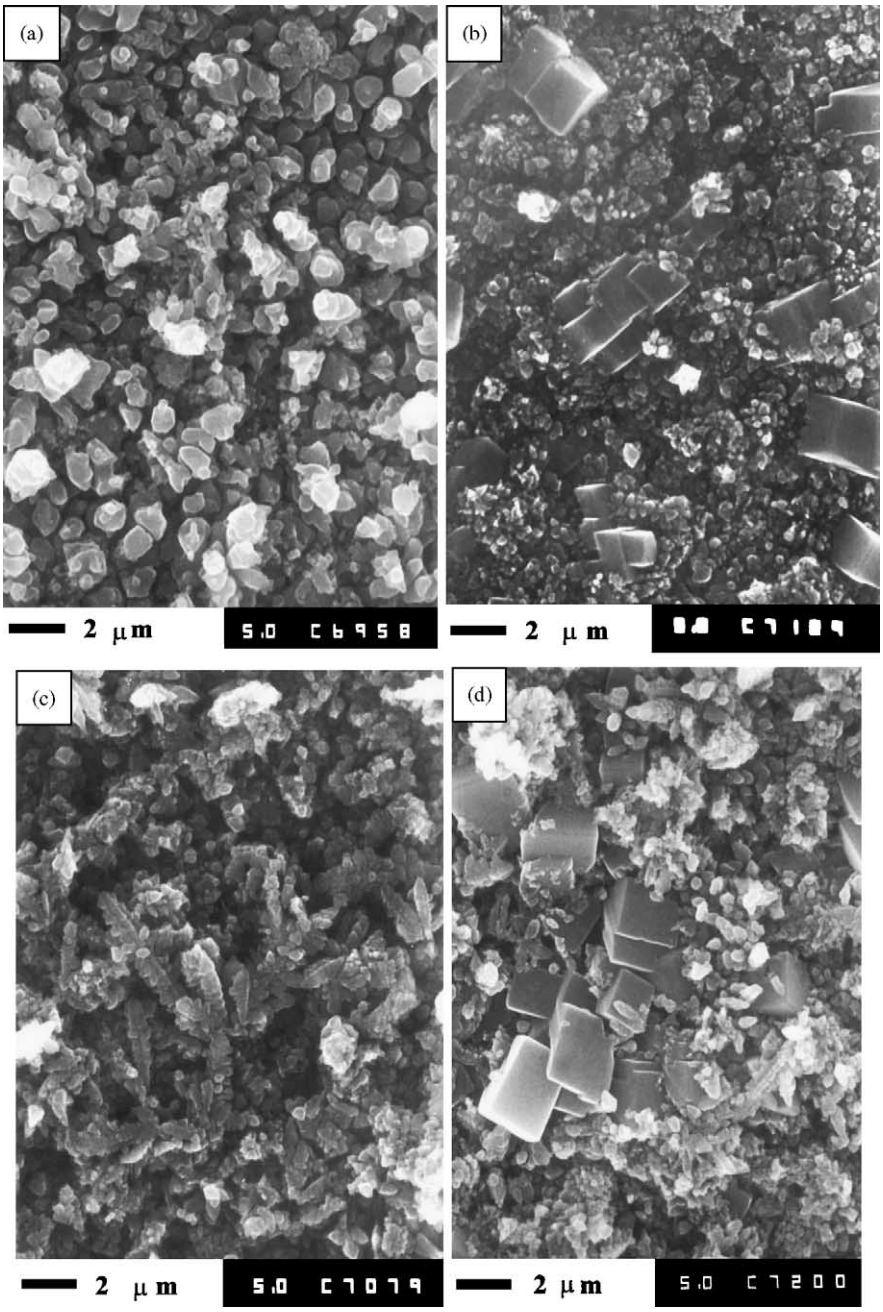

Fig. 16. Anodic layer formed after 16 h of cycling of a $Pb/PbO_2/PbSO_4$ electrode in 0.05 M H_2SO_4 solution at potential scan rate 2 mV/s (a and b) and 4 mV/s (c and d). Electrode polarization was stopped at 1600 mV (a and c) and at 700 mV (b and d).

concentration is similar in profile to the curves giving the dependence of the electrochemical activity of PbO_2 (Fig. 1) and of the βPbO_2 content in the anodic layer (Fig. 2) on the concentration of the H_2SO_4 solution. This similarity gives us grounds to assume that the latter two dependences are influenced by the concentration of the HSO_4^- ions in the solution. The greatest amount of βPbO_2 is found in the anodic layer formed within the acid concentration region in which the concentration of HSO_4^- ions is the highest. Hence, the concentration of HSO_4^- ions determines the formation of βPbO_2. It is within this acid concentration region that the lead dioxide electrode has the highest electrochemical activity.

To be able to understand the influence of the ions of the solution on the electrochemical activity of the PbO_2 phase we should consider the structure of the PbO_2 particles.

4.2. Composition and structure of PbO_2 particles and agglomerates

Lead oxides always react with water forming hydrated surface layers. Lead dioxide particles comprise crystal (PbO_2)

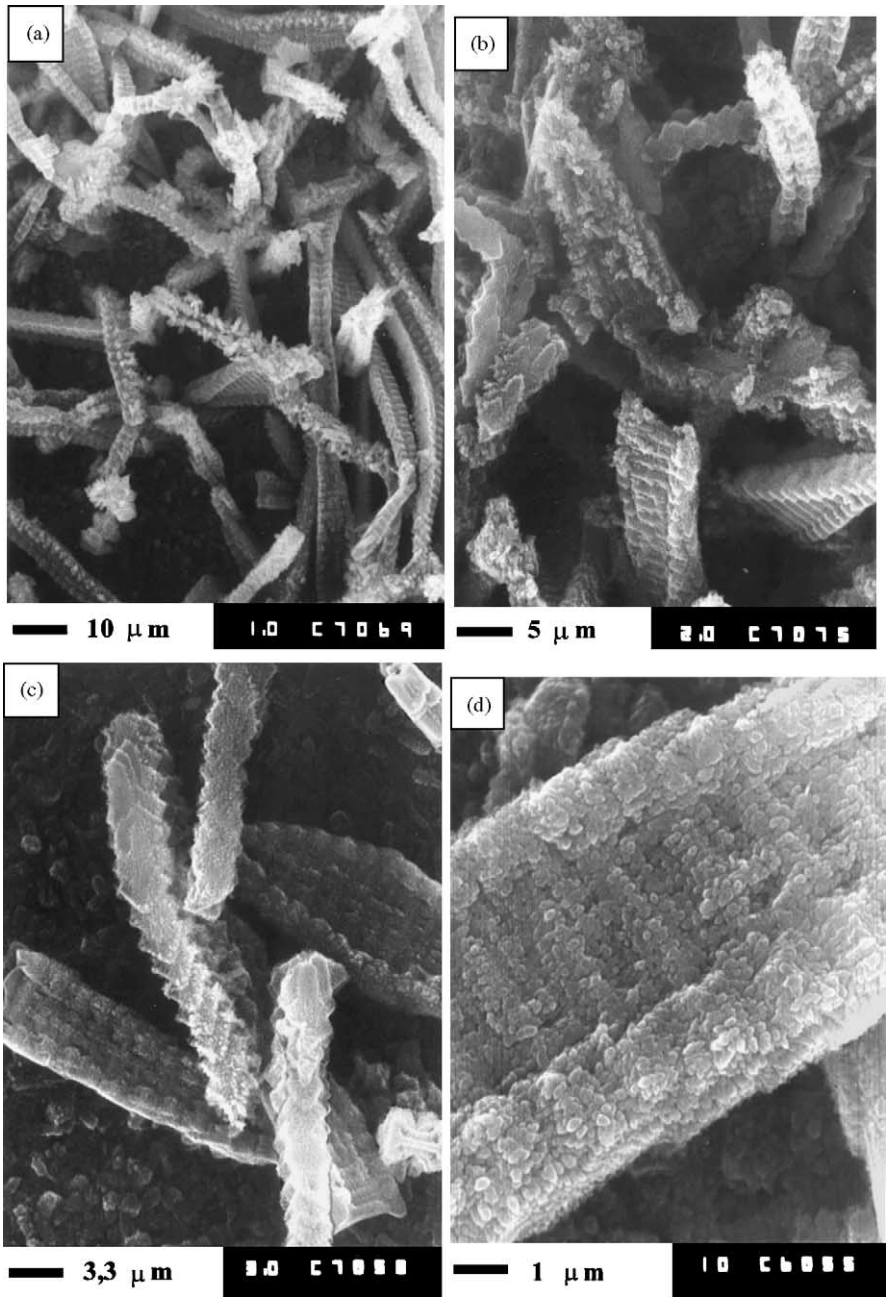

Fig. 17. Structure of the anodic layer formed after 16 h of cycling of a $Pb/PbO_2/PbSO_4$ electrode in 0.05 M H_2SO_4 solution at scan rate 10 mV/s (a and b) and 20 mV/s (c and d). Electrode polarization was stopped at 1600 mV.

and hydrated (gel) zones ($PbO(OH)_2 \cdot xH_2O$) [17,31]. The crystal part consists of orthorhombic αPbO_2 and/or tetragonal βPbO_2 crystallites. The crystal and gel zones in the particles are in equilibrium. Another equilibrium exists also between the gel zones' composition and the ions of the solution [11]. $PbO(OH)_2$ has amphoteric properties (H_2PbO_3) and can exchange both cations and anions with the solution [11]. This makes the PbO_2 particles and agglomerates an open system. (For the sake of simplicity, we will refer to this system as "PbO_2 particles".) Hence, the composition of the solution will affect the composition and structure of the gel and crystal zones as well as the proportion between them, which was also evidenced by XRD investigations in ref. [11]. Through shifting the equilibrium crystal ↔ gel zones in one direction or the other, PbO_2 particles of different shapes are formed.

(a) When the ions of the solution contribute to increasing the volume of the crystal zones at the expense of the gel zones, the PbO_2 particle acquires crystal shape (Figs. 7,8,16,17).
(b) When the ions of the solution facilitate the increase of the gel zones in the PbO_2 particle, the latter's shape is drop-like or spherical (globular) (Figs. 4 and 10–13).

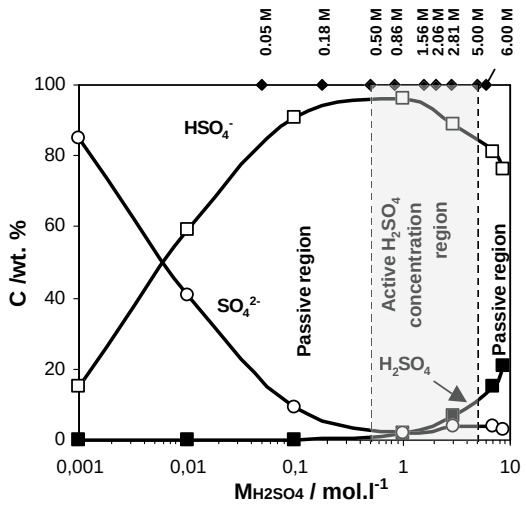

Fig. 18. Concentration of SO_4^{2-} and HSO_4^- ions resulting from the dissociation of H_2SO_4 vs. H_2SO_4 concentration [26–30].

The reactions of PbO_2 reduction proceed in active centers located in the hydrated (gel) zones [32]. Hence, the electrochemical activity of the lead dioxide will depend on the ratio crystal/gel zones and on the concentration of active centers in the gel zones.

4.3. Processes of PbO_2 reduction and effect of sulfuric acid ions on these processes

The PbO_2 particles interconnect into agglomerates, aggregates and skeleton. Their crystal zones are also interconnected. The crystal zones are degenerated semi-conductors [33] with electron conductivity, i.e. they conduct the current from the current collector to the site of the electrochemical reaction (active center) and in the opposite direction. For the electrochemical reaction of PbO_2 reduction to proceed in a given active center, it is necessary that both electrons and protons reach this center. This may happen in the gel zones of the particles. If charges of one type only (electrons or H^+ ions) reach the active center, the latter will be charged electrically and so will the whole gel zone. Consequently, the reaction will stop. For the reaction to proceed, the charges of the gel zone should be neutralized, which is achieved by attracting electrical particles with the opposite charge to enter the gel zone.

The gel zones are both ion conductive and electron conductive, and thus provide the transfer of H^+ ions from the solution to the active centers and of electrons from the crystal zones to the active centers and in the opposite direction. The following reaction of PbO_2 reduction proceeds in the active centers:

$$PbO(OH)_2 + 2H^+ + 2e^- \rightarrow Pb(OH)_2 + H_2O \quad (5)$$

The water formed as a result of this reaction dilutes the gel zones. $Pb(OH)_2$ gets in contact with the sulfuric acid and a reaction of sulfation proceeds:

$$Pb(OH)_2 + HSO_4^- + H^+ \rightarrow PbSO_4 + 2H_2O \quad (6)$$

If the crystal zones predominate in the particles, the volume of the gel zones is small and the number of active centers is small, too, and so is the number of PbO_2 particles that can be reduced. Hence, the lead dioxide has low electrochemical activity, i.e. low capacity.

If the gel zones predominate greatly in the particle, its electrochemical activity is somewhat reduced because of the impeded electron transport. Only a definite proportion between the crystal and gel zones in the PbO_2 particles make them electrochemically active [31]. The greater the number of particles with optimum ratio between gel and crystal zones, the higher the capacity of the $PbO_2/PbSO_4$ electrode. Based on the gel-crystal model for the structure of the PbO_2 particles, the influence of HSO_4^- ions on the electrochemical activity of these particles can be explained as follows. At H_2SO_4 concentrations from 5.0 to 0.5 M, the equilibrium between the HSO_4^- ions in the gel zones and in the solution maintains optimum proportion between the gel and crystal zones in the particles. The latter are drop-like in shape, i.e. they contain substantial volume of gel zones. The concentration of active centers in these particles is high and hence the electrochemical reaction of PbO_2 reduction proceeds at a high rate. The high concentration of HSO_4^- ions in the solution keeps up the optimum ratio between the gel and crystal zones in a maximum number of PbO_2 particles that are in contact with the solution. Hence, the capacity of the $PbO_2/PbSO_4$ electrode is high.

In the passive region with the lowest H_2SO_4 concentration, the content of SO_4^{2-} ions in the solution increases at the expense of the reduced concentration of HSO_4^- ions. This leads to the formation of αPbO_2 phase in the particles and its content increases on diluting the solution, whereas the content of the βPbO_2 phase diminishes (Fig. 2). On sweeping the potential at a high rate, dendrites of crystal-like particles are formed (Figs. 15 and 17). At low potential scan rate, crystal shaped PbO_2 particles are formed (Fig. 16a and b). These particles contain small volume of gel zones and hence their electrochemical activity is low (Fig. 1).

In the passive region of high H_2SO_4 concentrations, the concentration of H_2SO_4 molecules in the solution increases, while that of the HSO_4^- ions decreases (Fig. 18). PbO_2 particles with crystal-like shape (Figs. 7 and 8) of the αPbO_2 modification (Fig. 2) are formed. The βPbO_2 content decreases.

The two passive regions have the following features in common: crystal-shaped PbO_2 particles, reduced volume of the gel zones and hence lower concentration of active centers in these zones, increased content of the αPbO_2 phase, smaller number of PbO_2 particles that can be reduced and consequently, lower capacity of the $PbO_2/PbSO_4$ electrode (Fig. 1).

4.4. Influence of ions in the H_2SO_4 solution on the processes of oxidation of the $PbSO_4$ crystals in the active region of H_2SO_4 concentrations

If we compare the data for the solubility of $PbSO_4$ crystals as a function of the H_2SO_4 concentration (Fig. 3) with those for the concentration of HSO_4^- ions in the solution (Fig. 18), we can see that $PbSO_4$ has the highest solubility within the region of high concentration of HSO_4^- ions in the solution. Figs. 9 and 10 show that, in this concentration region, $PbSO_4$ crystals are oxidized through metasomatic processes. The oxidation of $PbSO_4$ must result in the formation of HSO_4^- ions. This may happen if the following reaction proceeds:

$$PbSO_4 + 3H_2O \rightarrow PbO(OH)_2 + HSO_4^- + 2e^- + 3H^+ \quad (7)$$

HSO_4^- and H^+ ions get into the solution and drop-like $PbO(OH)_2$ particles are formed. This reaction may proceed on those parts of the $PbSO_4$ surface where electrons can pass from the $PbSO_4$ crystal to the lead dioxide phase and through it to the current collector.

In the drop-like particles, a reaction of dehydration and formation of βPbO_2 crystal zones proceeds. The following equilibrium is established:

$$PbO(OH)_2 \Leftrightarrow \beta PbO_2 + H_2O \quad (8)$$

Fig. 9 shows that, at 2.81 M H_2SO_4 concentration, the $PbSO_4$ crystals are covered, completely or partially, with a lead dioxide layer that grows inside the volume of the $PbSO_4$ crystals forming oriented endotaxial layers of PbO_2 particles. The microstructure of these layers can be seen in Figs. 9b and 10c and d. The mechanism of disintegration of these layers into individual PbO_2 particles or rows of particles can be observed in Figs. 10d and 11e and f. During the subsequent electrode discharges, $PbSO_4$ crystals are formed at different sites and of different shape and size than the primary $PbSO_4$ crystals. Thus, the primary PbO_2 aggregates disintegrate into a porous mass of shapeless agglomerates and aggregates. The electrode is electrochemically active and its life depends on the strength of the bonds between the individual agglomerates and aggregates. Such processes take place in the positive active mass, too, whereby its initial structure formed during plate formation, changes into a new structure during cycling [35].

4.5. Oxidation of $PbSO_4$ crystals in the passive region of high H_2SO_4 concentrations

As evident from Figs. 7 and 8, the PbO_2 particles formed in this acid concentration region are crystal shaped and of the αPbO_2 species; some unoxidized $PbSO_4$ remains in the anodic layer as well (Fig. 2). In this case, the oxidation of the $PbSO_4$ crystals involves less water and follows the reaction:

$$PbSO_4 + 2H_2O = PbO(OH)(HSO_4) + 2e^- + 2H^+ \quad (9)$$

Further reactions proceed in two directions, the first one being the formation of αPbO_2:

$$PbO(OH)(HSO_4) \rightarrow \alpha PbO_2 + H_2SO_4 \quad (10')$$

and the second one is the interaction with water:

$$PbO(OH)(HSO_4) + H_2O = PbO(OH)_2 + H_2SO_4 \quad (10'')$$

The latter two reactions result in the formation of particles with gel and crystal zones. The gel zones contain some $PbO(OH)(HSO_4)$ molecules which probably reduce considerably their electron and ion conductivity as well as the number of active centers in them. The electrochemical activity of the $PbO_2/PbSO_4$ electrode declines substantially.

The picture in Fig. 7a evidences that αPbO_2 crystal-shaped particles arrange in the volume of the $PbSO_4$ crystal being oxidized in such a way that the shape of the obtained agglomerate is rough and differs from the shape of the initial $PbSO_4$ crystal. This type of PbO_2 agglomerates differ from those presented in Figs. 9–12, which indicates that the oxidation of the $PbSO_4$ crystal to PbO_2 agglomerate proceeds via a different mechanism.

4.6. Oxidation of $PbSO_4$ crystals in the passive region of low H_2SO_4 concentrations

Figs. 13–17 show that, in this acid concentration region, there is no similarity in shape of the $PbSO_4$ crystals and PbO_2 aggregates. This implies that the processes of oxidation of $PbSO_4$ to PbO_2 involve a step during which the Pb^{2+} ions pass through the solution prior to being oxidized to Pb^{4+} ions.

In analogy to the mechanism of the processes of electrochemical reduction of the metal ions and formation of the metal crystal lattice during electroplating, the following stages of the process of oxidation of $PbSO_4$ to PbO_2 can be assumed for this particular case:

(i) Dissolution of the $PbSO_4$ crystal through the reaction

$$PbSO_4 = Pb^{2+} + {SO_4}^{2-}$$

(ii) Diffusion of the Pb^{2+} and ${SO_4}^{2-}$ ions from the $PbSO_4$ surface to the bulk of the solution. ${SO_4}^{2-}$ ions are stable in this acid concentration region (Fig. 18).

(iii) Depending on the pH of the solution, Pb^{2+} ions may form a number of complexes with OH-ions [12,34].

(iv) Adsorption of the Pb^{2+} complexes or Pb^{2+} ions on the surface of the lead dioxide particles and agglomerates and their diffusion until they reach an active center on the surface or into the interior of the gel zones, where the two-valent Pb^{2+} ions or complexes will be oxidized to four-valent ones.

(v) Hydration of the four-valent Pb^{4+} ions or rearrangement of the hydrated complexes and their incorporation into the lead dioxide particles, or nucleation and growth of new lead dioxide particles. At this stage the lead dioxide particle grows or a new particle is formed.

(vi) Interconnection of the lead dioxide particles into agglomerates or aggregates. The hydrated layers of the lead dioxide particles interconnect and an interaction is established between the crystal and gel zones within an agglomerate. If the interaction between the particles building the agglomerate is weak, they shed off. If the interparticle interaction is strong, whereby an equilibrium is established between all gel and crystal zones throughout the agglomerate, they build a strong skeleton.

The above processes are much more complicated than the process of reduction of the metal ions, as they involve building of the structure of a compound, and probably the above elementary processes are not the only ones. All these processes will be influenced both by the H_2SO_4 concentration and by the potential scan rate. As the H_2SO_4 solution is highly diluted and not buffered, the changes in potential may lead to the formation of a diffusion layer at the PbO_2 surface with a different pH than that of the bulk solution, which will have a considerable effect on the formation of complexes. At 0.18 M H_2SO_4 concentration and potential scan rate of 100 mV/s, flat lead dioxide particles are formed sized about 100 nm (Fig. 13e and f) or cylindrical agglomerates (Fig. 13b and c) comprising layers of PbO_2 particles with dimensions about 80–100 nm. When the H_2SO_4 concentration is 0.05 M and the potential scan rate is >10 mV/s, long lead dioxide dendrites are formed (Figs. 15 and 17).

The dendrites illustrated in Fig. 17a and b (at 10 mV/s) and Fig. 17c and d (at 20 mV/s) feature step-like crystal forms built up of ordered individual particles. It can be assumed that the structure of the lead complexes does exert a strong influence on the agglomerates' shape of the newly formed phase. Generally, lead(II) complexes contain various Pb^{2+} and OH^- ions (for example $[Pb_4(OH)_4]^{4+}$, $[Pb_6(OH)_8]^{4+}$, etc.), whose structure is transferred to the new phase during the oxidation of Pb^{2+} to Pb^{4+}. Thus, the newly formed particles may have a shape influenced by the structure of the initial Pb^{2+} complexes. An interesting fact is that PbO_2 particles of nano-sizes arrange in crystal-shaped agglomerates (Fig. 17).

4.7. Determining the maximum amount of H_2SO_4 that can take part in the discharge reactions in the lead-acid battery without causing disintegration or passivation of PAM

In a previous investigation of ours we have established that within a certain H_2SO_4 concentration region part of the anodic layer sheds off [6]. Fig. 19 presents this dependence of the amount of shed off anodic layer after 16 h of electrode cycling in H_2SO_4 solutions of various concentrations. It can be seen that the most intense shedding of particles and aggregates is observed in the acid concentration region from 1.5 M H_2SO_4 (1.095 s.g.) to 0.5 M H_2SO_4 (1.030 s.g.). In order to guarantee long cycle life of the lead-acid cell, not limited by shedding of PAM, the H_2SO_4 concentration

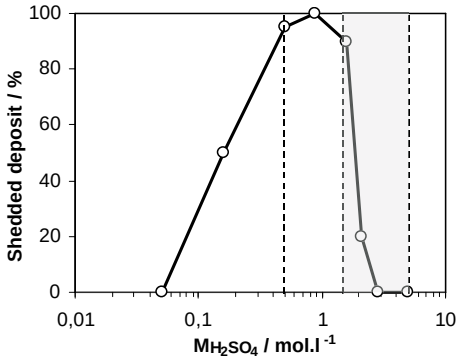

Fig. 19. Shedding of the anodic layer as a function of H_2SO_4 concentration [6].

should not fall down below 1.5 M H_2SO_4. Hence, there is a lower limit of the decrease of the acid concentration during discharge. The upper acid concentration limit is 5 M H_2SO_4, above which the region of passivation of the $PbO_2/PbSO_4$ electrode starts. Thus, the working interval within which the concentration of the H_2SO_4 solution may change on cycling is from 5.0 M H_2SO_4 (1.28 s.g.) to 1.5 M H_2SO_4 (1.10 s.g.), i.e. 3.5 M H_2SO_4 per 1 l of H_2SO_4 solution with s.g. 1.28 takes part in the reactions on both battery plates.

It is well known that Sb, Sn and Bi ions have a beneficial effect on the cycle life of lead-acid batteries [36]. The proposed model for the processes in the PbO_2 particles can explain the mechanism of influence of the above ions. This model could help in finding new more efficient additives to the electrolyte, which would improve the performance of the batteries.

The capacity of the positive plate may decline as a result of local passivation or disintegration of the PAM structure in the plate interior when the H_2SO_4 concentration enters one of the two passive concentration regions. In order to guarantee the reversibility of the PAM structure during charge and discharge, the H_2SO_4 concentration in the PAM pores should be maintained within the above mentioned limits. This can be achieved through an appropriate ratio between the quantities of the four active materials (Pb, PbO_2, H_2SO_4 and H_2O) in the lead-acid cell and the densities of PAM and NAM.

References

[1] Z. Takehara, K. Kanamura, Electrochim. Acta 29 (1984) 1643.
[2] Z. Takehara, K. Kanamura, J. Electrochem. Soc. 134 (1987) 13.
[3] Z. Takehara, K. Kanamura, J. Electrochem. Soc. 134 (1987) 1604.
[4] P. Ekdunge, D. Simonsson, J. Electrochem. Soc. 132 (1985) 2529.
[5] A. Czerwinski, M. Zelazowska, M. Grden, K. Kuc, J.D. Milewski, A. Nowacki, G. Wojcik, M. Kopczyk, J. Power Sources 85 (2000) 49.
[6] B. Monahov, D. Pavlov, A. Kirchev, S. Vasilev, J. Power Sources 113 (2003) 281.
[7] G.W. Vinal, D.N. Craig, J. Res. Bur. Stand. 22 (1939) 55.
[8] V. Danel, V. Plichon, Electrochim. Acta 27 (1982) 771.
[9] I.G. Kiseleva, B.N. Kabanov, Dokl. Akad. Nauk SSSR 122 (1956) 1042.

[10] G.A. Kokarev, V.A. Kolesnikov, M.Ya. Fioshiu, Elektrokhimiya (Russ.) 19 (1983) 196.
[11] D. Pavlov, I. Balkanov, J. Electrochem. Soc. 139 (1992) 1830.
[12] R.N. Sylva, P.L. Brown, J. Chem. Soc. Dalton Trans. (1980) 1577.
[13] S. Hattori, S. Tosano, O. Kusuoku, Denki Kagaku 44 (1976) 109.
[14] D.B. Mathews, M.A. Habib, S.P.S. Badwal, Aust. J. Chem. 34 (1981) 247.
[15] K. Asai, M. Tsubota, K. Yonezu, K. Ando, J. Power Sources 7 (1981) 73.
[16] P. Eckdunge, D. Simonsson, J. Electrochem. Soc. 132 (1985) 2521.
[17] D. Pavlov, I. Balkanov, T. Halachev, P. Rachev, J. Electrochem. Soc. 136 (1989) 3189.
[18] Merck—Tabellen fur das Labor, 44 pp.
[19] S.C. Barnes, R.T. Mathieson, in: D.H. Collins (Ed.), Batteries 2, Prengamon Press, Oxford, 1965, p. 41.
[20] D. Pavlov, E. Bashtavelova, J. Electrochem. Soc. 131 (1984) 1468.
[21] D. Pavlov, E. Bashtavelova, J. Electrochem. Soc. 133 (1986) 241.
[22] D. Pavlov, Electrochim. Acta 23 (1978) 845.
[23] D. Pavlov, Z. Dinev, J. Electrochem. Soc. 127 (1980) 855.
[24] D. Pavlov, Electrochim. Acta 13 (1968) 2051.
[25] T.F. Young, L.A. Blatz, Chem. Rev. 44 (1949) 93–115.
[26] A.K. Covington, I.V. Dobson, W.F.K. Wynne-Jones, Trans. Faraday Soc. 61 (1965) 2050–2057.
[27] H.M. Dawson, Proc. Leeds Soc. 2 (1929-1934) 359–364.
[28] A.J. de Bethune, T.S. Licht, N. Swendeman, J. Electrochem. Soc. 106 (1959) 616–625.
[29] T.F. Young, Rec. Chem. Prog. 12 (1951) 81–95.
[30] H. Bode, in: R.J. Brodd, K.V. Kordesch (Eds.), Lead-Acid Batteries, John Wiley & Sons, New York, 1977, p. 46.
[31] D. Pavlov, J. Electrochem. Soc. 139 (1992) 3075.
[32] D. Pavlov, G. Petkova, J. Electrochem. Soc. 149 (5) (2002) A 654.
[33] W. Mindt, J. Electrochem. Soc. 116 (1969) 1076.
[34] Qi. Liu, Y. Lin, J. Colloid Interf. Sci. 268 (2003) 266.
[35] D. Pavlov, G. Petkova, M. Dimirtov, M. Shiomi, M. Tsubota, J. Power Sources 87 (2000) 39.
[36] D. Pavlov, J. Power Sources 33 (1991) 221.